Characterization of natural copper ore as oxygen carrier in chemical-looping with oxygen uncoupling of anthracite

Haibo Zhao *, Kun Wang, Yanfei Fang, Jinchen Ma, Daofeng Mei, Chuguang Zheng

State Key Laboratory of Coal Combustion, Huazhong University of Science and Technology, Wuhan 430074, PR China

ARTICLE INFO

ABSTRACT

Chemical-looping with oxygen uncoupling (CLOU) provides a novel route for CO_2 capture with low energy penalty. In this paper, natural copper ore, known for its low cost and abundant supply, was examined as an oxygen carrier material for CLOU in a batch fluidized-bed reactor. The relations between oxygen release/uptake rates and reactor temperatures were first explored. It was found as a general trend that both the oxygen release and uptake rates increase with the reactor temperature. The CLOU thermo-chemical characteristics were further investigated comprehensively using a typical Chinese anthracite (GaoPing coal) as fuel. The effects of reactor temperature, superficial fluidization velocity, oxygen carrier to fuel ratio, coal particle size, and steam content in fluidization gas on carbon conversion rate, coal combustion efficiency, and gas yields were investigated. It was found that the following factors would lead to a higher carbon conversion rate: a higher reactor temperature, smaller superficial fluidization velocity, smaller coal particle size, larger ratio of oxygen carrier to fuel, and higher steam volume concentration in the fluidization gas. High combustion efficiency above 96% and CO_2 yield above 0.95 were attained in these tests. The copper ore particles showed only slight agglomeration and sintering in the long-term operation.

1. Introduction

Carbon capture and storage (CCS) has been widely accepted as an important way to reduce anthropogenic emission of greenhouse gas into the atmosphere (IPCC, 2008). However, current state-of-the-art CCS technologies usually involve large-scale gas separation. In the three approaches of CO_2 capture from coal-derived power generation including pre-combustion capture technologies, post-combustion capture technologies and oxy-combustion technologies, CO_2 and/or O_2 separation is required, which leads to a high economic cost and energy penalty inherent to these CO_2 capture approaches (Figueroa et al., 2008). Different from the combustion principle (Lyon and Cole, 2000), chemical-looping combustion (CLC) (Ishida and Jin, 1996) avoids completely any gas separation and enables the production of a concentrated CO_2 stream through circulating solid oxygen carrier (OC) particles (which supply active lattice oxygen for fuel combustion) between air reactor (AR) and fuel reactor (FR).

In the in situ gasification chemical-looping combustion (iG-CLC) (Adanez et al., 2012; Fan et al., 2012), the FR is usually fluidized by steam, CO_2 or mixtures of these gases. The fluidization gas also acts as a gasifying agent to gasify the remaining char in the iG-CLC system. The OC reacts with volatiles and gas products from coal pyrolysis and gasification. However, the char gasification in this system is usually a rate-limiting step. If the residence time of char particles in the FR is not sufficiently long, the char particles will pass to the AR, reducing the CO_2 capture efficiency and coal combustion efficiency (Berguerand and Lyngfelt, 2008; Leion et al., 2009a; Shen et al., 2009).

Recently, chemical-looping with oxygen uncoupling (CLOU) was proposed as a new CLC technology, in which a special OC was used to release gaseous O_2 in the FR to avoid the rate-limiting gasification step in the iG-CLC process (Mattisson et al., 2009a). The schematic of CLOU process is presented in Fig. 1. In the FR, several reactions (i.e. reaction (R1)–(R4)) take place nearly simultaneously (Adanez et al., 2012). Since the FR is a high-temperature and oxygen-deficient environment, some oxidized OC (for example, CuO, Mn_2O_3, Co_3O_4, and some perovskite-type oxides) decomposes into the reduced OC and gaseous O_2. At the same time, coal devolatilizes to produce char and volatiles. Then these combustibles are burnt immediately. It is worth noting that in the CLOU system coal does not have to gasify first in the FR since the oxygen release of OC and the combustion of char are usually far faster than the gasification of char. Thereby, a higher overall reaction rate in the FR is attained, leading to much less OC inventory and lower circulation rate, and much

---
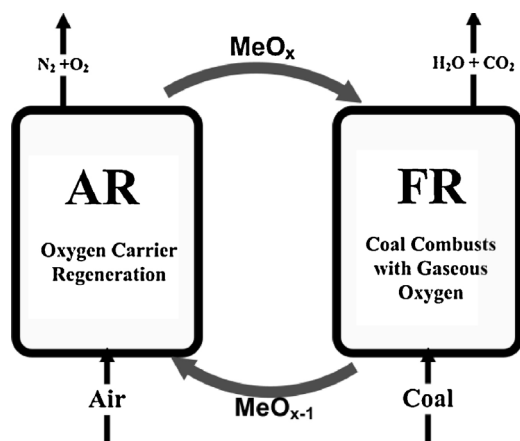
Fig. 1. The schematic of CLOU system.

higher carbon conversion, CO_2 capture efficiency and combustion efficiency.

$$MeO_x \leftrightarrow 2MeO_{x-1} + O_2(g) \tag{R1}$$

$$Coal \rightarrow char + volatiles(g) + H_2O(g) \tag{R2}$$

$$Char + O_2(g) \rightarrow CO_2(g) \tag{R3}$$

$$Volatiles(g) + O_2(g) \rightarrow CO_2(g) + H_2O(g) \tag{R4}$$
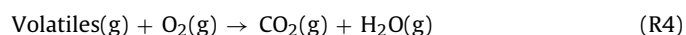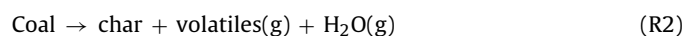
In the CLOU technology, the OC has to decompose to release gaseous oxygen in the FR and regenerate itself in the AR at temperatures of interest for combustion (800–1200 °C). The CLOU concepts have been demonstrated in the batch-operating laboratory-scale fluidized-bed reactors (Arjmand et al., 2012; Gayan et al., 2012; Shulman et al., 2009) and continuously operating interconnected fluidized-bed reactors (Abad et al., 2012; Adanez-Rubio et al., 2013) using synthesized metal oxides systems (CuO/Cu$_2$O, Adanez-Rubio et al., 2011, 2012a; Leion et al., 2009b; Mattisson et al., 2009b; Moldenhauer et al., 2012; Mn$_2$O$_3$/Mn$_3$O$_4$, Azimi et al., 2011; Ryden et al., 2011a; Shulman et al., 2011; and perovskite-type oxides, Leion et al., 2009c; Ryden et al., 2011b) as OC and methane, kerosene, coal or petroleum coke as fuel. Among these OCs, Cu-based oxides have received a great deal of attention due to the advantages of high reactivity, high oxygen transport capacity, and suitable oxygen equilibrium partial pressure. The Cu-based oxides are also favored for their stable recyclability of oxygen release and uptake, exothermicity for fuel combustion in the FR and environmental friendliness relative to Co-based OC.

Regarding the use of copper oxides for CLOU process, most of the investigations were concentrated on synthesized Cu-based OCs. In Sweden, Mattisson et al. (2009a, 2009b) first investigated the reaction between the CuO/ZrO$_2$ OC synthesized by freeze granulation and petroleum coke in a fluidized-bed reactor. It was found that the average reaction rate of petroleum coke is accelerated 50 times in the CLOU in comparison to the reaction rate of the same fuel with an iron-based OC in the CLC. Leion et al. (2009b) further investigated the oxygen release ability of the CuO/ZrO$_2$ OC and its CLOU reactivity with six different solid fuels. In addition, Moldenhauer et al. (2012) demonstrated for the first time the CLOU of liquid fuel (kerosene) using manganese-based and copper-based OC materials in a 300 W circulating fluidized-bed laboratory reactor and Arjmand et al. (2011) investigated the reactivity of CuO/Al$_2$O$_3$ and CuO/MgAl$_2$O$_4$ in the CLOU using methane. In the research group of ICB-CSIC, a comprehensive screening study reviewing 25 different Cu-based OCs was carried out by Adanez-Rubio et al. to select suitable materials for CLOU process (Adanez-Rubio et al., 2011; Gayan et al., 2012). The OCs with 60 wt% of CuO on MgAl$_2$O$_4$ and with 40 wt% of CuO on ZrO$_2$ from mechanical mixing following

by pelletizing by pressure were identified as suitable materials for CLOU process. Based on this, Abad et al. (2012) and Adanez-Rubio et al. (2012a) investigated the reaction between bituminous coal and CuO/MgAl$_2$O$_4$ OC synthesized by spray drying in a 1.5 kWth continuously operated CLOU system. Coal combustion efficiency of nearly 100%, high carbon capture efficiency (above 0.97), high char conversation in the FR (above 0.94), and fast char conversion rate (7–33%/s) were obtained under a wide range of operating conditions. Then, Adanez-Rubio et al. (2012b, 2013) identified three CLOU operational regions for this CuO/MgAl$_2$O$_4$ OC with different OC to coal mass ratios (higher than 50, in the range 50–25, below 25) and investigated the relation between the coal rank and the performance of the CLOU process using the CuO/MgAl$_2$O$_4$ OC. In our previous experiments, Mei et al. (2013a, 2013b) prepared the CuO/CuAl$_2$O$_4$ OC with high copper contents (60 wt% CuO) by sol–gel and investigated its oxygen release/uptake characteristics and CLOU reactivity with three typical Chinese coals with different coal ranks in a batch fluidized-bed reactor. It was found that the higher the coal rank was, the lower the reaction rate was.

According to the studies reviewed above, the synthetic Cu-based OCs exhibited excellent performances in various reactors for different fuels, which are attributed to their controllable chemical composition and physical structure. However, the synthetic OCs also have a number of disadvantages such as high preparation cost, long preparation period, and small preparation batch. As known, for a continuously operated CLOU system with a carbon separation system of 90% efficiency to reach a CO_2 capture efficiency of 95%, it requires 45, 85, 140 and 490 kg OC particles per MW thermal power when using lignite, medium volatile bituminous, low volatile bituminous and anthracite, respectively (Adanez-Rubio et al., 2013). Manufacturing OC prepared by pure chemicals results in too high cost to be used in the large-scale chemical-looping plants. On the contrary, the preparation process may accompany considerable pollutant emission. For example, when preparing the CuO/CuAl$_2$O$_4$ OC by sol–gel (Mei et al., 2013b), the copper nitrate and the aluminum isopropoxide were used as precursors for Cu and Al elements in the OC. The considerable pollutant emission of NO_x will be produced in the process of calcination in the air-atmosphere which cannot ignore during the production of this synthetic OC. In comparison to the synthetic CuO-based OCs, natural copper ore has the advantages of low cost and rich reserves as the materials used in CLOU system. However, copper ore with complicated composition may exhibit relatively low reactivity. Up to date, there are very few works in the literature for CLOU process dealing with the use of copper ore.

Recently, only Wen et al. (2012) investigated three kinds of natural copper ore particles in terms of cyclic oxygen release and uptake. The copper ores were tested in a thermogravimetric analyzer (TGA) and fluidized bed rector to explore their reactivity, stability and agglomeration behavior. It was found that the natural copper ore particles with a low Cu content (only 5.82 wt% CuO) did not agglomerate during the first 20 cycles at a very high temperature of 980 °C. However, serious agglomeration was observed in copper ore particles with higher Cu content (63.25 wt% and 87.28 wt% CuO). Therefore, special attention should be paid to the agglomeration and sintering of copper ore particles at high temperatures.

Considering that there is no publication on the study of nature copper ore with coal, this study focuses on the feasibility of natural copper ore with moderate Cu content as OC in the CLOU process. The oxygen release and uptake of the copper ore particles and the CLOU reactivity of low-volatile anthracite were explored in a batch fluidized-bed reactor. The effects of reactor temperature, superficial fluidization velocity, OC to fuel ratio, coal particle size, and steam content in fluidizing gas on coal conversion rate, coal combustion efficiency, and gas yields were examined.

Table 1
Copper ore compositional characterization.

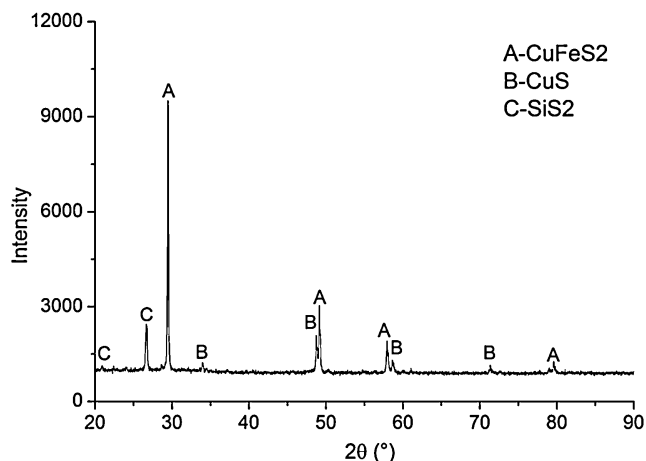| Samples	Component analysis (wt%)					Ultimate analysis (wt%)					
	CuO	CuFe$_2$O$_4$	SiO$_2$	CaSO$_4$	Al$_2$O$_3$	Cu	Fe	Si	Ca	S	Al
Before calcination	–	–	–	–	–	35.49	25.44	3.22	0.53	34.22	1.12
After calcination	21.04	70.05	5.53	2.29	1.08	48.88	45.00	3.55	0.93	0.85	0.79

Fig. 2. XRD result of the copper ore after flotation.

Table 2
Physical and chemical properties of the fresh copper ore particles.

CuO content (wt%)	44.39
Oxygen transport capacity, R_{OC} (wt%)	4.44
Specific surface area, BET (m^2/g)	0.217
Particle size (mm)	0.125–0.180
Density (kg/m^3)	5353
Crushing strength (N)	1.53
XRD main phases	CuO, CuFe$_2$O$_4$

Table 3
Proximate and ultimate analyses of GP coal.

Proximate analysis (wt%, ad)		Ultimate analysis (wt%, daf)	
Moisture	2.25	C	70.04
Volatiles matter	10.69	H	3.54
Ash	20.62	N	1.90
Fix char	66.44	S	1.24
Low heating value (MJ/kg)	26.17		

2. Experimental

2.1. Preparation and characterization of copper ore OC particles

The natural copper ore from Zhongtiaoshan (China) was selected as material for OC. The original copper oxide ores, which generally have a lower copper content and are difficult for flotation, usually undergo the sulfuration reaction before the flotation process, which changes copper oxide in the original ore to copper sulfide and greatly improves the surface hydrophobicity (Xiong and Zheng, 2013). The sodium sulfide and xanthate are used as vulcanizing and collecting agent, respectively, in the flotation process. The XRD result (see Fig. 2) of the copper ore sample after the flotation shows that this copper ore mainly consists of CuFeS$_2$, CuS and SiS$_2$, while CuO or Fe$_2$O$_3$ phase is not found.

In order to generate desired CuO and CuFe$_2$O$_4$, improve the mechanical strength and eliminate the inherent sulfur in the ore, the original ore was calcined for 5 h at 500 °C and then 10 h at 1000 °C in an air-atmosphere muffle oven. This procedure of calcination has been verified by some experiments that it can eliminate almost all of the sulfur in the ore. Ultimate analysis and composition analysis of the raw ore particles and the calcined ones were performed by X-ray fluorescence (XRF) spectrometry (EDAX EAGLE III), as shown in Table 1. It is shown that the raw ore contained a large amount of sulfur before calcination but the amount of sulfur was greatly reduced after calcination. Therefore, the amount of released SO$_2$ in calcination, which has an effect on environment, should not be ignored and an additional process is needed to absorb these SO$_2$.

The calcined ore was then crushed and sieved to 0.125–0.180 mm to obtain the fresh OC particles. Table 2 shows the physical and chemical properties of the fresh OC particles (after calcination). The BET surface area of the particles was evaluated by N$_2$-absorption method (Micromeritics, ASAP2020). The real density was measured by an automatic true density analyzer (AccuPyc 1330). The crushing strength was determined by a crushing strength apparatus (Shimpo FGJ-5) from 20 measurements. The crystalline phases were determined by X-ray diffraction

(XRD, X'Pert PRO) analysis. It can be found that the OC is mainly composed of CuO and CuFe$_2$O$_4$ that can release gaseous oxygen in the FR (Siriwardane et al., 2013; Wang et al., 2011). The ratio of CuO/CuFe$_2$O$_4$ is about 0.3. The surface morphology of the OC particles was examined in an Environment Scanning Electron Microscope (ESEM, FEI Quanta 200).

2.2. Preparation and characterization of coal particles

Typical anthracite from GaoPing (GP coal) in China was used as the fuel. The proximate and ultimate analyses of the anthracite are presented in Table 3. The original coal was first dried at 105 °C for 10 h and then ground and sieved to different diameter ranges of 0.125–0.2 mm, 0.2–0.3 mm and 0.3–0.4 mm to obtain the fuel particles.

2.3. Batch fluidized bed reactor and experimental procedures

All the tests were carried out in a batch fluidized-bed reactor, as shown in Fig. 3, which is composed of a gas feeding unit, a fluidized-bed reaction unit, and a gas detecting unit. The gas feeding unit
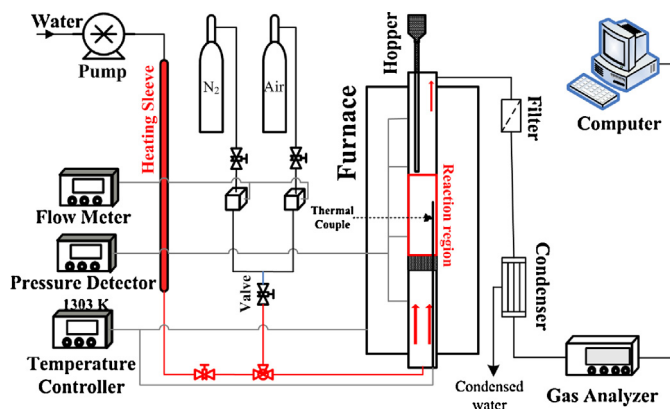

Fig. 3. An overview of the fluidized-bed reaction system.

Table 4
Main operational conditions for experimental tests in the fluidized bed reactor.

Test	T_{upt} (°C)	T_{rel} (°C)	Q_{in, N_2} (mL/min)	Q_{in, H_2O} (mL/min)	m_{oc} (g)	Ω_{OC} (m_{coal} (g))	d_{coal} (mm)
Oxygen uptake and release experiments							
UR01	600	900	600	–	30	–	–
UR02	700	925	600	–	30	–	–
UR03	800	950	600	–	30	–	–
UR04	900	975	600	–	30	–	–
UR05	950	1000	600	–	30	–	–
CLOU experiments of GP coal							
CLOU01	–	900	800	–	40	2.7 (0.3)	0.2–0.3
CLOU02	–	850	800	–	40	2.7 (0.3)	0.2–0.3
CLOU03	–	950	800	–	40	2.7 (0.3)	0.2–0.3
CLOU04	–	900	600	–	40	2.7 (0.3)	0.2–0.3
CLOU05	–	900	700	–	40	2.7 (0.3)	0.2–0.3
CLOU06	–	900	800	–	40	4.0 (0.2)	0.2–0.3
CLOU07	–	900	800	–	40	2.0 (0.4)	0.2–0.3
CLOU08	–	900	800	–	40	2.7 (0.3)	0.105–0.18
CLOU09	–	900	800	–	40	2.7 (0.3)	0.3–0.4
CLOU10	–	900	640	160	40	2.7 (0.3)	0.2–0.3
CLOU11	–	900	480	320	40	2.7 (0.3)	0.2–0.3
CLOU12	–	900	320	480	40	2.7 (0.3)	0.2–0.3

provides air, or nitrogen, or gas mixture of nitrogen and steam to simulate the AR or FR atmosphere, respectively. The fluidized-bed reaction tube has a length of 890 mm and an inner diameter of 26 mm, which is surrounded by an electrical furnace. A porous plate was placed in the tube at a distance of 400 mm from the bottom. The temperature of the reactor was measured with K-type thermocouples located 10 mm above the porous plate. Particle materials including coal and OC were introduced to the reaction tube from the hopper located on the top of the reactor. The off gas from the top of the reactor was first introduced into a filter to remove particulate matter carried by gas, and then into an electric cooler to remove the steam. The gas was then led to an on-line gas analyzer (Gasboard Analyzer 3100) to measure the concentrations of CO_2, CO, CH_4, H_2 and O_2.

The reactor was operated first to investigate the oxygen uptake/release characteristics of the copper ore and then to simulate the CLOU process. The operation conditions for oxygen uptake/release and CLOU tests are presented in Table 4. The OC to fuel ratio, Ω_{OC} was defined as the ratio of the oxygen provided by OC to the oxygen required for the full combustion of coal. A value of $\Omega_{OC} = 1$ corresponds to the stoichiometric flow of CuO and $CuFe_2O_4$ needed to fully convert coal to CO_2 and H_2O, being CuO and $CuFe_2O_4$ reduced to Cu_2O and $CuFeO_2$. Thus, Ω_{OC} was calculated with the following equation:

$$\Omega_{OC} = \frac{R_{OC} m_{OC}}{\Phi_{coal} m_{coal}} \tag{1}$$

m_{OC} and m_{coal} are the mass of OC and coal added into the reactor. Φ_{coal} is the stoichiometric kilogram of oxygen to convert 1 kg of coal to CO_2 and H_2O.

For investigating the oxygen release process, the reactor was first heated to the set-point temperature in N_2 atmosphere. Then, 30 g completely oxidized OC were added into the reactor by the hopper to investigate the oxygen release of the OC. The oxygen uptake process occurs as the fluidization gas was switched from N_2 to air. Then, the reduced OC absorbed oxygen from air and finally the oxygen concentration of the fluidization gas increased to 20.95%, which marked the end of the oxygen uptake process. With regard to the CLOU process, 40 g OC and 0.2–0.4 g anthracite were used. The copper ore particles were first exposed to air for 30 min at a set-point temperature to ensure complete oxidation. Then, the fluidization gas was rapidly switched to N_2 or the mixture of N_2 and steam, which led to a quick drop of the O_2 partial pressure in the reactor. When the O_2 partial pressure dropped below the corresponding equilibrium partial pressure of the OC at

the set-point temperature, copper ore particles began to release gaseous oxygen. Once a stable oxygen concentration was achieved, the coal particles were added into the hopper and pushed into the reactor by a pressurized purging nitrogen gas. The fuel was assumed to be completely burnt out until no CO_2 was detected in the exhaust gas. Afterwards, the fluidization gas was switched to air to regenerate the reduced OC. The influences of the following factors on the thermo-chemical performance of this copper ore in the CLOU process were investigated: reactor temperatures ranged between 850 and 950 °C, fluidization flows ranged between 600 and 800 mL/min, OC to fuel ratio within 2–4, coal particle sizes with different diameter ranges and steam concentration in the fluidization agents from 0% to 60%.

3. Data evaluation

The OC conversion rates (X_{red} for oxygen release and X_{ox} for oxygen uptake) were calculated by measuring the mole concentrations of O_2 leaving the reactor:

$$X_{red} = \int_{t_1}^{t} \frac{Q_{out} y_{O_2,out}}{n_{O_2}} \, dt \tag{2}$$

$$X_{ox} = \int_{t_2}^{t} \frac{1}{n_{O_2}} (Q_{in} y_{O_2,in} - Q_{out} y_{O_2,out}) \, dt \tag{3}$$

Here, Q_{in} is the inlet flow rate and Q_{out} is the molar flow rate of the exhaust gas leaving the reactor; $y_{O_2,in}$ and $y_{O_2,out}$ are the O_2 concentrations in the fluidizing and exhaust gases, respectively; t_1 and t_{red} are the start time and end time of the oxygen release process, t_2 and t_{ox} are the start time and end time of oxygen uptake process; and n_{O_2} is the moles of molecular oxygen that can be released from the fully oxidized OC.

In a real interconnected fluidized reactor, there may be not possible for the OC to absorb and release oxygen completely in the reactors. Therefore, the average OC conversion rates in the oxygen uptake (until the conversion rate reaches 95%) and release (until the conversion rate reaches 65%) processes were, respectively, defined as Eqs. (4) and (5), which was used to evaluate the conversion rates of OC in a real CLOU unit.

$$x_{0.95, \, upt} = \frac{0.95}{t_{0.95, \, upt} - t_2} \times 100\% \tag{4}$$

$$x_{0.65, \, rel} = \frac{0.65}{t_{0.65, \, rel} - t_1} \times 100\% \tag{5}$$

Here, $t_{0.95,upt}$ and $t_{0.65,rel}$ represent the points in time when the OC conversion rates reach 95% (for oxygen uptake) and 65% (for oxygen release), respectively.

In the CLOU process, the conversion rate of combustible carbon in reduction period, $X_{C,comb}$, and average conversion rate, $x_{0.95,C}$, were calculated as follows:

$$X_{C,comb} = \frac{\int_{t_0}^{t} F_{flus}(y_{CO} + y_{CO_2} + y_{CH_4}) \, dt}{\int_{t_0}^{t_{total}} F_{flus}(y_{CO} + y_{CO_2} + y_{CH_4}) \, dt} \quad (6)$$

$$x_{0.95,C} = \frac{0.95}{t_{0.95,C} - t_0} \times 100\% \quad (7)$$

Here, y_{CO}, y_{CO_2} and y_{CH_4} are the molar fraction of CO, CO_2 and CH_4 in the gas products, F_{flus} is the molar flow rate of the gas in the outlet, determined by N_2 balance between the inlet and the outlet of the reactor. t_0, t_{total} and $t_{0.95,C}$ represent the start time, the end time and the point in time when the carbon conversion rate reaches 95%, respectively.

In order to further study the CLOU process, gas yields of each component exiting the reactor, γ_i were calculated as follows:

$$\gamma_i = \frac{\int_{t_0}^{t_{total}} [y_i F_{flus}] \, dt}{\int_{t_0}^{t_{total}} [(y_{CO} + y_{CO_2} + y_{CH_4}) F_{flus}] \, dt} \quad (8)$$

Here, y_i is the molar fraction of the component i (include CO_2, CO, CH_4 or H_2) in the product gas. Especially, γ_{H_2} could be understood as the ratio of hydrogen to carbon in the flue gas.

Finally, the coal combustion efficiency in the reactor, η_{eff}, was used to measure the utilization degree of the heat of the anthracite. In Eq. (9), CH_4, CO and H_2 in the flue gas are considered as thermal loss.

$$\eta_{eff} = 1 - \left(\frac{H_{CO} \int_{t_0}^{t_{total}} M_{CO} F_{flus} y_{CO} \, dt + H_{CH_4} \int_{t_0}^{t_{total}} M_{CH_4} F_{flus} y_{CH_4} \, dt + H_{H_2} \int_{t_0}^{t_{total}} M_{H_2} F_{flus} y_{H_2} \, dt}{m_{coal} H_{coal}} \right) \quad (9)$$

Here, H_{CO}, H_{CH_4}, H_{H_2} and H_{coal} are the lower heating value of CO, CH_4, H_2 and coal, respectively; M_{CO}, M_{CH_4} and M_{H_2} represent the molar mass of CO, CH_4 and H_2.

4. Results and discussions

4.1. Oxygen uptake and release of copper ore

Reactor temperature and equilibrium oxygen partial pressure are the main influencing factors for the oxygen uptake/release of OC in the CLOU (Mattisson et al., 2009a). Here, we first investigated the effect of reactor temperature on the performance of the oxygen uptake/release of the natural copper ore.

4.1.1. Oxygen release

In this section, the oxygen release experiments were conducted at five set-point temperatures ranged in 900–1000 °C, as shown in Table 4 (UR01–UR05). Fig. 4 shows the O_2 concentration profiles at different temperatures. A small amount of O_2 was released within 20–50 s and a lower O_2 concentration was observed at a higher temperature. Following the small peak of oxygen concentration, the major concentration peak of O_2 emerged. With the increase of temperature, the major O_2 concentration peak first increased obviously (900–950 °C) and then decreased slightly (950–1000 °C). This is attributed to the occurrence of sintering or agglomeration of copper ore particles at a higher temperature of more than 950 °C (which inhibits the reactivity of OC particles).

However, it is still unknown that which component (CuO or $CuFe_2O_4$) caused the first stage of the oxygen release. Thus, an additional experiment in the fluidized-bed reactor was carried out to
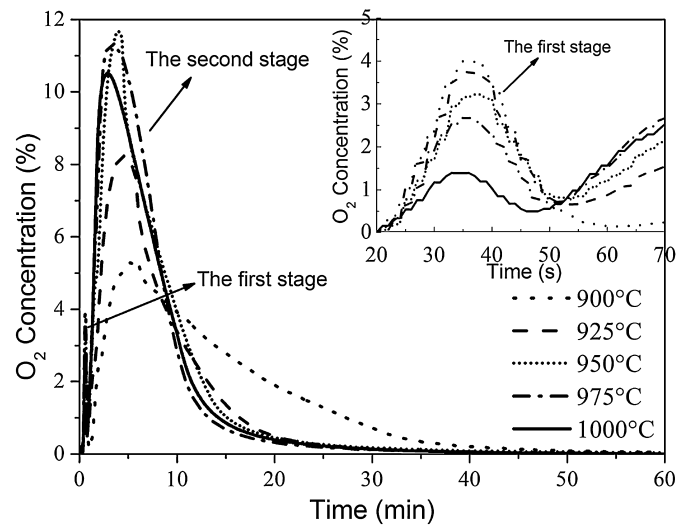
Fig. 4. Oxygen concentrations at different temperatures in oxygen release tests.

further identify the first oxygen release period. The experimental procedure is as follows: the reactor is first heated to 900 °C in a N_2 atmosphere; then 30 g completely oxidized OC is added into the reactor by the hopper; after about 90 s, turn off the electrical furnace and the temperature of the reactor decreases rapidly; when the O_2 concentration decreases to zero, it is assumed that this experiment is finished. Afterwards, the copper ore particles were analyzed by XRD to identify the crystalline phases. It can be found in the XRD pattern (see Fig. 5) that a small amount of Cu_2O was observed after the experiment and no $CuFeO_2$ or Fe_2O_3 was observed in the particles. This result indicates that the CuO component in the surface of the copper ore particles released oxygen faster than the $CuFe_2O_4$ when the copper ore was added into the reactor, and the first peak of the oxygen concentration was caused by the oxygen release of the external CuO of the particles. Moreover, the difference of the peak oxygen concentration for the first stage may be attributed to the sintering of CuO which easily occur in the high temperature. The higher the temperature was, the more
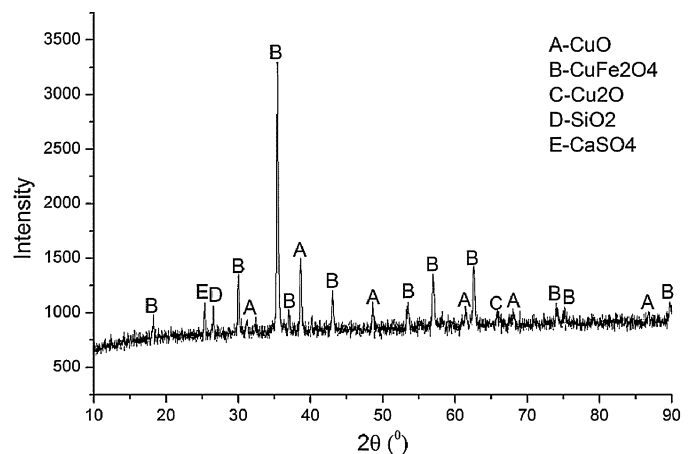
Fig. 5. XRD result of the copper ore particles after the additional oxygen release experiment.
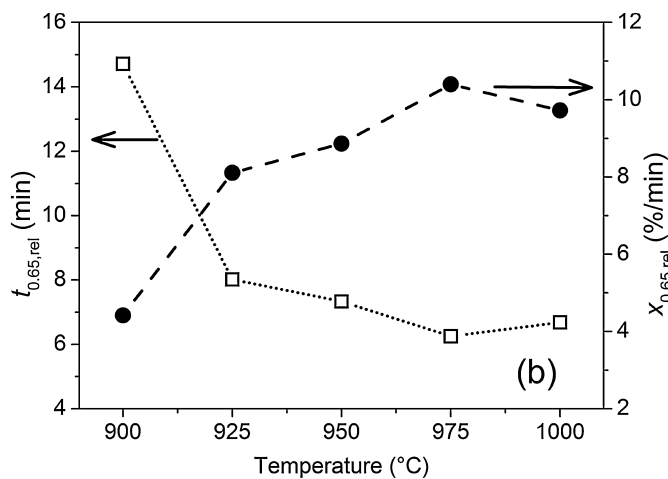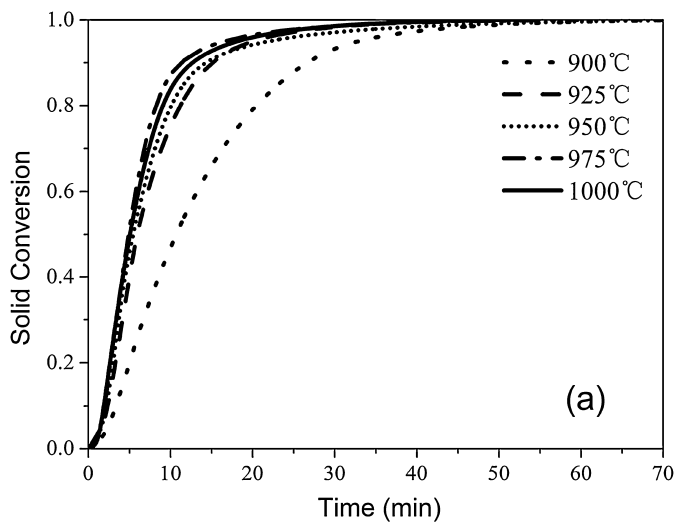
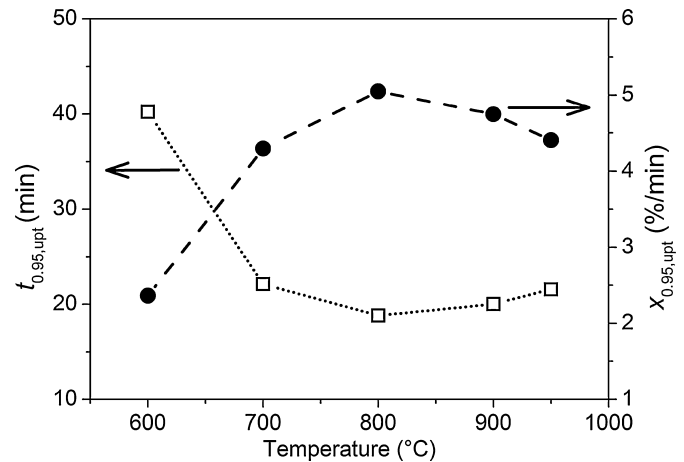Fig. 6. Effect of the oxygen release temperature on the reactivity of OC.

Fig. 7. Effect of the oxygen uptake temperatures on the reactivity of OC.

average OC conversion rate $x_{0.95,upt}$ increased from 2.4%/min to 4.4%/min. A peak value of 5.1%/min for $x_{0.95,upt}$ was observed at 800 °C, i.e. it took less than 19 min for the OC conversion rate to reach 0.95. However, when the reactor temperature was higher than 700 °C, the variation of OC conversion rate was very slight. Accordingly, temperatures from 700 °C to 950 °C were appropriate for the oxygen uptake processes.

4.2. CLOU performance of GaoPing anthracite

The CLOU process was carried out in the fluidized bed reactor using the copper ore as OC and GP anthracite as fuel. The possible influencing factors including the FR temperature, superficial fluidization velocity, OC to fuel ratio, coal particle size, and steam content in fluidization gas were studied, and their effects on the coal conversion rate, coal combustion efficiency, and gas yields were investigated. In addition, successive reduction–oxidation cycles were carried out at 900 °C to study the potential cyclic stability of the natural copper ore in CLOU of anthracite.

4.2.1. Redox cycle test

It was reported that in the CLC processes using iron ore as OC and coal as fuel, the reactivity of iron ore is not stable in the first several redox tests (Adanez et al., 2010; Cuadrat et al., 2012). The unstable performance of natural iron ore may be attributed to its unstable physical structures such as pore structures and its unstable chemical components. Five reduction–oxidation cycles were carried out in a batch fluidized-bed reactor to analyze the stability of the natural copper ore. The operation conditions of CLOU01 are presented in Table 4, and the total operation time was about 10 h.

As shown in Fig. 8, the average carbon conversion rate, $x_{0.95,C}$, dropped from 4.1%/min in the first reduction period to about 3.3%/min in the second reduction, and tended to be stable in the rest of reduction processes. It can be concluded that only one redox cycle is required to stabilize the copper ore OC. Factually, when the fresh OC particles were utilized in the CLOU, their specific surface area, which largely determined the reactivity of the OC, was reduced probably because of the blocking of fly ash generated in the coal combustion process and a slight sintering in the OC particle surface. More physiochemical characterizations will be presented in Section 4.3 to support the argument.

During the five redox tests, the yield of CO_2 was the highest (above 0.97), followed by CO (about 0.02), CH_4 and H_2, suggesting that a nearly full conversion of coal to CO_2 was achieved. As a result, high combustion efficiency (above 96%) was also obtained. The gas yields were relatively stable, while the combustion efficiency
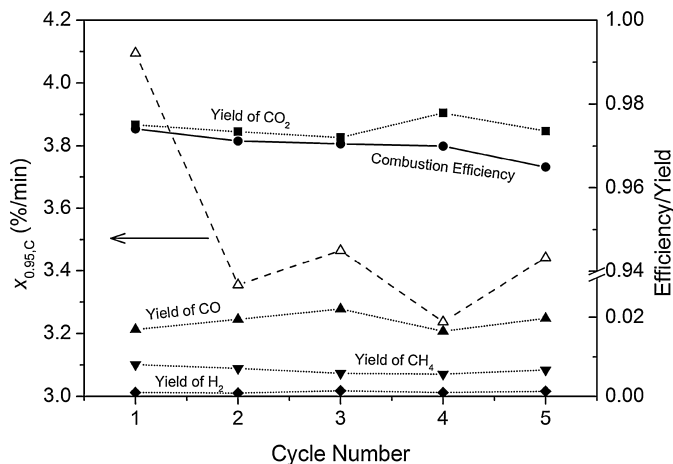
serious sintering occurred for the CuO phase. Therefore, a lower O_2 concentration was observed at a higher temperature. As shown in Table 1, it can be seen that the CuO content is about 21% in the fresh OC. But, it is obviously found in Fig. 4 that the amount of the oxygen released by the first peak was far smaller than the theoretical amount of oxygen from CuO decomposition. Therefore, the second peak of the oxygen concentration could be caused by the oxygen released of the interior CuO and $CuFe_2O_4$ of the particles.

Fig. 6 shows the effects of the reactor temperature on the OC conversion, the characteristic time $t_{0.65,rel}$ and the average conversion rate $x_{0.65,rel}$. As shown in Fig. 6a, a higher temperature generally led to a higher conversion rate (see $x_{0.65,rel}$ and $t_{0.65}$ in Fig. 6b), except that the conversion rate at 1000 °C was slightly lower than that at 975 °C. As the reactor temperature increased from 900 °C to 1000 °C, $t_{0.65}$ decreased gradually from 14.7 min to 6.3 min. It is found that when the reactor temperature is higher than 925 °C $t_{0.65}$ tends to be steady. 925–975 °C could be selected as the temperature operation window for the oxygen release process.

4.1.2. Oxygen uptake

The oxygen uptake experiments (marked as UR01–UR05 in Table 4) at different temperatures ranged in 600–950 °C were then carried out. Fig. 7 shows the effects of the reactor temperatures on oxygen uptake process. With the temperature increasing from 600 °C to 950 °C, the characteristic time $t_{0.95,upt}$ for oxygen uptake decreased from 40.2 min to 21.6 min, and the corresponding

Fig. 8. Average carbon conversion rate, yields of gases and combustion efficiency for different cycle numbers.

Fig. 10. Average carbon conversion rate, yields of gases and combustion efficiency at different temperatures.

decreased slightly with the cycle number, suggesting that the reactivity of the copper ore OC decreased slightly in the redox tests. Generally, it is observed that the cycle number has little influence on the thermo-chemical performance of the CLOU once the copper ore particles are stabilized after the first redox, which demonstrates that the copper ore is potentially suitable for long-term use in the CLOU process.

4.2.2. Effects of reactor temperature

A group of experiments (CLOU01–CLOU03, see Table 4) operating at temperatures of 850 °C, 900 °C and 950 °C were carried out in the fluidized-bed reactor. Typical gas concentration profile of the reduction and oxidation processes in the CLOU is shown in Fig. 9, where the reactor temperature is 900 °C. The OC was first exposed in air atmosphere to ensure full oxidation. After switching the fluidization gas from air to N_2, the oxygen partial pressure decreased rapidly from 20.95% to a value close to the equilibrium partial pressure. When the oxygen concentration decreased to about 5%, the coal particles were added into the reactor. The combustion of the coal led to a rapid increase of CO_2 concentration, rising up to its maximum of 6.1% within 40 s. Because of the insufficient residence time of combustible gases in the reactor, a small amount of CO, H_2 and CH_4 from coal pyrolysis escaped from the reactor before
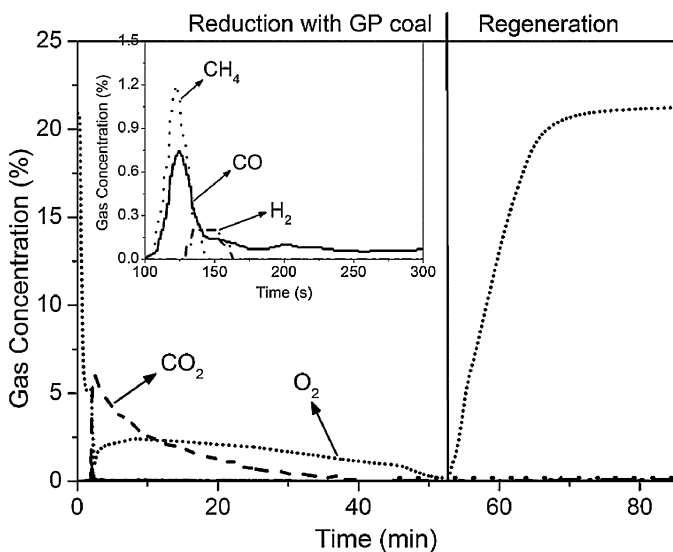

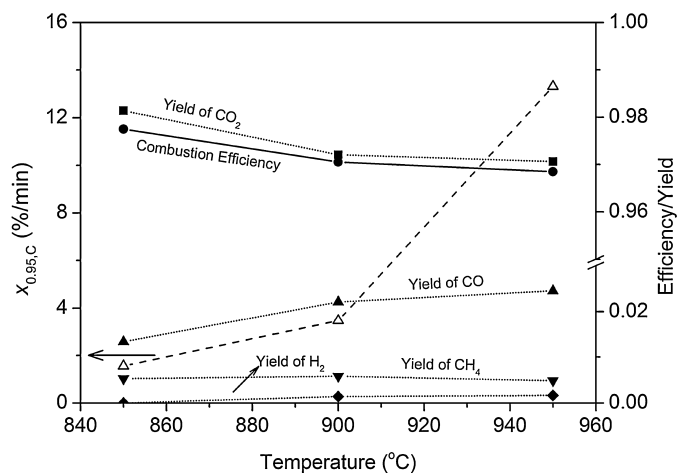Fig. 9. Gas concentration profile for a redox cycle at 900 °C.

combustion, which was considered as a thermal loss. The time required for the whole reduction process was about 40 min. Following the reduction, there was still some gaseous oxygen detected in the outlet, which indicated that excessive amount of OC was used. The reduced copper ore OC was then exposed to air to regenerate itself for a new cycle. No carbon-containing gas was detected in the reactor outlet during the oxidation process, suggesting that all of the coal particles were converted and no carbon deposited on the surface of OC particles in the reduction process.

The effects of reactor temperature on carbon conversion, gas yields, and combustion efficiency are shown in Fig. 10. The average carbon conversion rate, $x_{0.95,C}$, increased significantly with the increase of temperature. A higher coal combustion rate can be achieved at a higher temperature, which should be attributed a higher oxygen release rate of natural copper ore OC at a higher temperature (see Fig. 5). At 950 °C, $x_{0.95,C}$ was higher than 12%/min, i.e. it took less than 10 min to burn out 95% of the coal. With respect to the yields of H_2, CH_4 and CO, higher values can be obtained at higher temperatures, meaning that more combustible gases were not utilized at higher temperatures. As a result, the CO_2 yield and combustion efficiency decreased slightly as the reactor temperature increased. This problem could be overcome in a continuously operating CLOU unit which is capable of ensuring a sufficient amount of residence time for the volatiles for complete utilization (Adanez-Rubio et al., 2013).

However, it is noted that a certain degree of sintering was observed on the surface of the used OC at 950 °C. Factually, the reduction between copper oxide and carbon is exothermic, which results in an increase of real reactor temperature that favors more severe sintering of copper ore particles. Therefore, the set-point temperature of 900 °C was selected in the remaining CLOU tests.

4.2.3. Effects of the superficial fluidization velocity

Tests CLOU04–CLOU05 were carried out under different N_2 flow rates ranging from 600 mL/min to 800 mL/min (corresponding to the superficial gas velocities in m/s as 0.0741 m/s, 0.0865 m/s and 0.0988 m/s, which lead to $u/u_{mf} = 3.3$–6.9, 3.9–8.0, 4.4–9.2, where u_{mf} is the minimum fluidization velocity) to investigate the effects of the fluidization velocity. As shown in Fig. 11, a significant decrease in $x_{0.95,C}$ from 3.85%/min to 3.46%/min was observed with the increase of the N_2 flow rate. When the N_2 flow rates was 800 mL/min, higher yields of combustible gases including CH_4, H_2 and CO were achieved, which on the contrary led to the decrease of CO_2 yield as well as combustion efficiency. The effects of the superficial fluidization velocity can be mainly attributed to two factors:
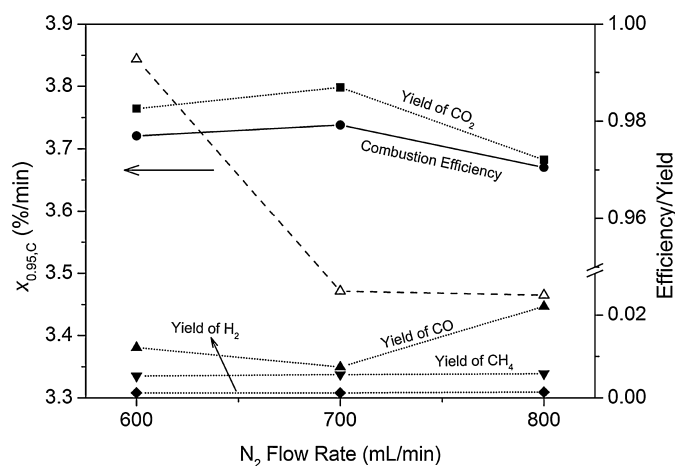
Fig. 11. Average carbon conversion rate, yields of gases and combustion efficiency for different N_2 flow rates.

Fig. 13. Average carbon conversion rate, yields of gases and combustion efficiency for different coal particle sizes.

(1) the larger bubbles formed under higher gas velocities reduced the contact area between fuel and gaseous oxygen, thereby leading to a lower reaction rate; (2) combustible gases escaped much faster from the reactor under higher gas velocity due to a shorter residence time in the reactor. The effects of superficial fluidization velocity found in this work agree well with the results of Son and Kim (2006) and Abad et al. (2010).

4.2.4. Effects of OC to fuel ratio

The OC to fuel ratio, Ω_{OC}, was defined as the ratio of oxygen provided by OC to the oxygen required for the full combustion of coal. The effects of Ω_{OC} on the CLOU performance were evaluated in tests CLOU01, CLOU06 and CLOU07, where the corresponding Ω_{OC} are about 2.7, 4.0 and 2.0, respectively.

As shown in Fig. 12, the $x_{0.95,C}$ increased linearly with the increase of Ω_{OC}. It means that less time is required for the complete conversion of the carbon in anthracite at higher Ω_{OC}. Furthermore, when using less coal, lower yields of CO, CH_4 and H_2 were observed. Thereby, an increasing trend of the yield of CO_2 and combustion efficiency was found. However, in the CLOU07 test with Ω_{OC} of 2.0, there was some CO_2 detected in the following oxidation process. The reason is that the oxygen provided by this OC was not enough for the complete combustion of the coal under the circumstance, resulting in some residual chars in the reduction period. Therefore, Ω_{OC} should be carefully selected to improve CO_2 purity

in the exhausts and enhance the combustion efficiency of coal in the FR.

4.2.5. Effects of coal particle size

The effects of the coal particle size were studied in CLOU08, CLOU01 and CLOU09, where the diameter ranges of coal particles were 0.105–0.2 mm, 0.2–0.3 mm and 0.3–0.4 mm, respectively. Fig. 13 shows the average carbon conversion rate, gas yields and combustion efficiency for different sizes of coal particles. The carbon conversion rate is highly dependent of the particle size. The $x_{0.95,C}$ coal conversion rates for particle ranges of 0.105–0.2 mm and 0.2–0.3 mm were nearly the same (about 3.3%/min). However, it decreased sharply to 1.7%/min for particle range of 0.3–0.4 mm. It can be concluded that large coal particles do not favor the combustion of char of high-rank anthracite due to limited contact between the gaseous oxygen and fuel particles. With the increase of coal particle size, more combustible gases were detected at the outlet. Thereby, a decreasing trend of the CO_2 yield was found. It is noted that a small amount of CO_2 was detected in the following oxidation process when using large coal particles of 0.3–0.4 mm, which was mainly ascribed to the slow reaction rate in the reduction. Still, high combustion efficiency (above 0.96) for the three tests was observed.

4.2.6. The effect of steam content

In the CLC processes, steam is usually used as a gasification agent reacting with solid fuel to improve the reaction rate (Leion et al., 2009a). In the CLOU processes, as the carbon conversion of anthracite is a little slow, steam was also introduced to accelerate the coal gasification and enhance the overall reaction rate in the reduction period. Three tests including CLOU10–CLOU12 with different steam contents in the fluidization gas were organized to examine the factor.

Compared with the experimental results obtained in test CLOU01 which did not use steam, the average carbon conversion rate significantly increased from 3.46%/min with steam volume concentration of 0–5.33%/min with steam volume concentration of 60%, as shown in Fig. 14. Obviously, the steam as a gasification agent can accelerate the conversion of solid char to gaseous CO and H_2, and these gasification products can more easily react with gaseous oxygen released by the OC. By increasing the steam content, the gasification reaction of the char was further enhanced. Meanwhile, more combustible gases escaped from the reactor, reducing CO_2 yield and combustion efficiency. These results suggest that it is effective to improve the reaction rate of the char by introducing steam into the CLOU reactor. Factually, in a real CLOU system, the
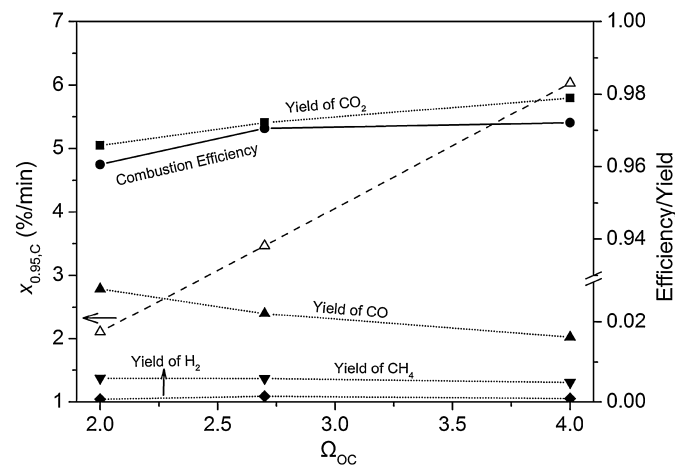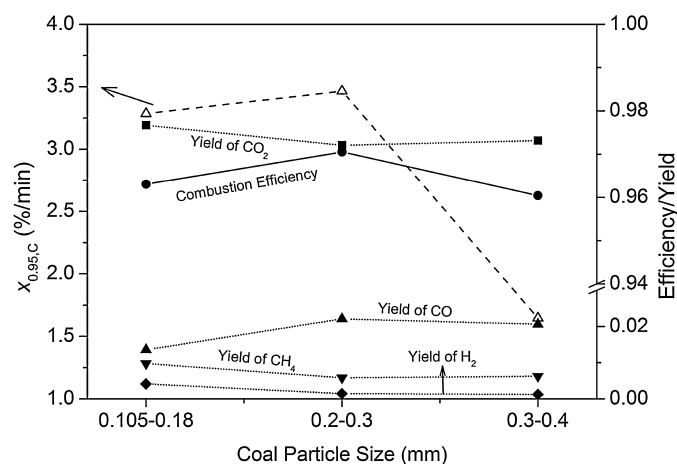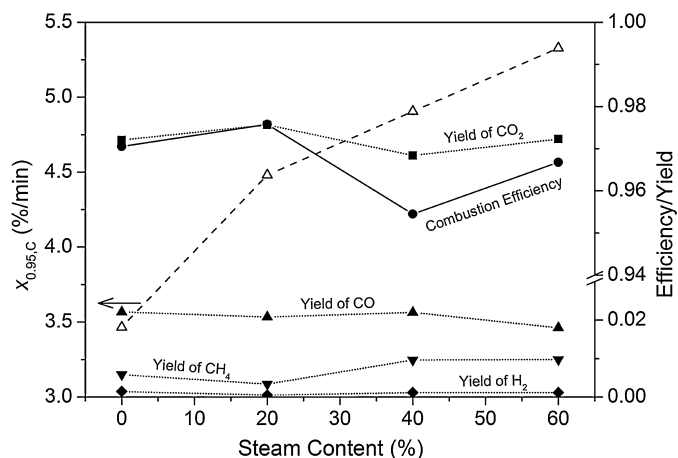

Fig. 12. Average carbon conversion rate, yields of gases and combustion efficiency for different OC to fuel ratios.

Fig. 14. Average carbon conversion rate, yields of gases and combustion efficiency for different steam contents.

Fig. 15. XRD results of the fresh OC (a), used OC in the oxygen uptake and release experiments (b), and used OC in the CLOU experiments (c).

steam could be produced by using the waste heat which can reduce the energy cost/penalization. It is worth noting that the steam content used in this technology is not necessarily too high as required in the iG-CLC. On the contrary, we also noted here a carbon separation system could increase the residence time of the anthracite char particles and therefore increase char conversion.

4.3. Characterization analysis of fresh and used copper ore OC

In this work, different batches of natural copper ore OC were used for different tests, and the longest time for continuous operation of a batch OC was about 10 h. For each batch of fresh copper ore OC, three redox cycles were completed to achieve its stable reactivity. The used OC particles in the oxygen uptake/release and CLOU tests were characterized by different techniques.

The crystalline phase compositions of the fresh copper ore OC samples, used OC after the oxygen uptake/release test and used OC
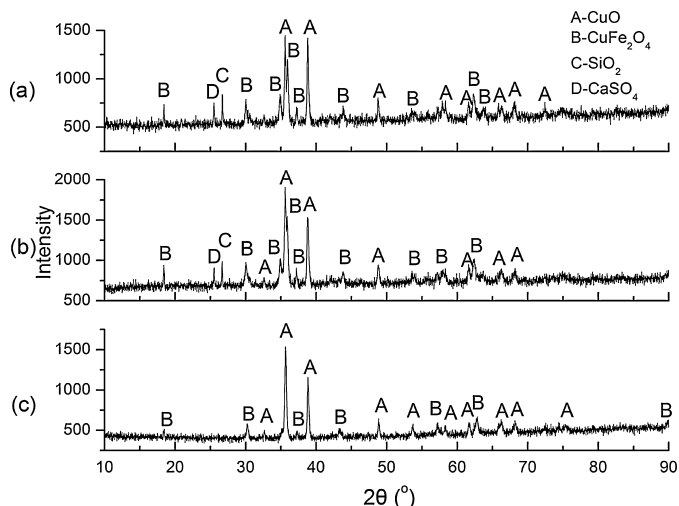
after the CLOU test were examined with XRD, as shown in Fig. 15. The major phases of all of the three samples were CuO and $CuFe_2O_4$. It seems that the $CuFe_2O_4$ was generated by CuO and Fe_2O_3 at high temperatures when the OC was calcined in muffle oven. No obvious change in the chemical composition of OC was observed. However, in the used OC after the CLOU tests, the phases SiO_2 and $CaSO_4$ were not observed in the XRD pattern (see Fig. 15c), as they might have interacted with the mineral composition of the coal ash.

Fig. 16 shows the SEM images of the fresh OC, used OC after the oxygen uptake/release experiments and used OC after the CLOU experiments. The fresh OC particles presented approximately spherical. Because of the attrition or slight agglomeration between larger particle and smaller fragment in the reaction, the used OCs exhibited obvious structural variation and were changed to irregular particles. To observe their surfaces, all the particles were
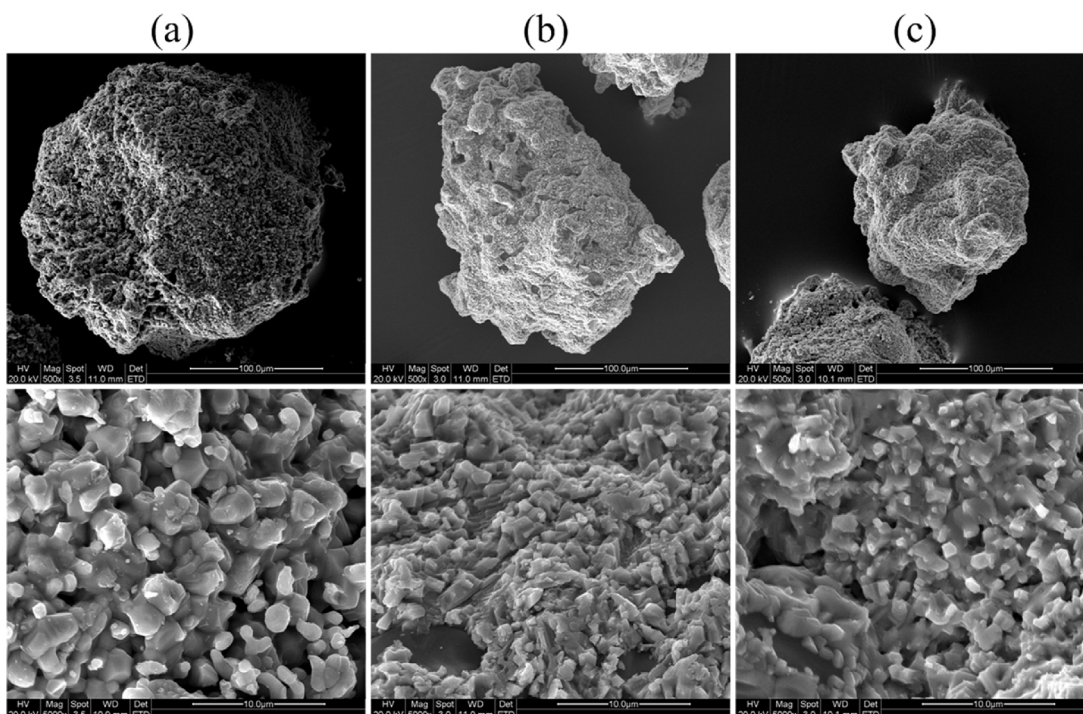

Fig. 16. SEM images of the fresh OC (a), used OC in the oxygen uptake and release experiments (b), and used OC in the CLOU experiments (c).

Table 5
Pore structure analysis of the OC particles.

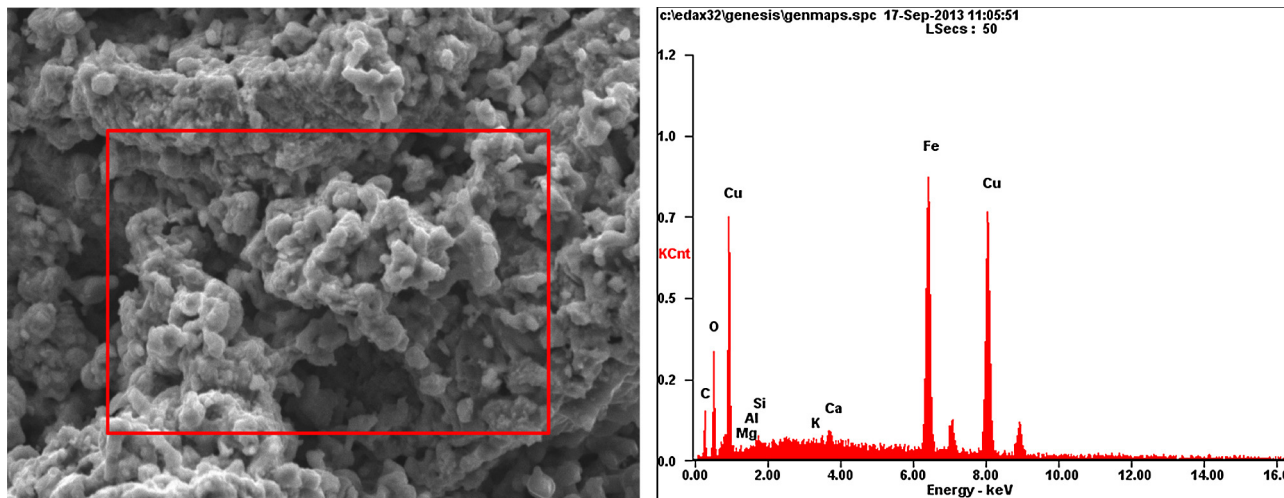| Samples	BET area (m²/g)	Pore volume (cm³/kg)	Average pore diameter (nm)
Fresh OC	0.217	0.46	8.68
After UR test	0.146	0.32	8.47
After CLOU test	0.115	0.31	10.70

Fig. 17. SEM-EDX analysis of the used copper ore particles after CLOU test.

further enlarged to observe the porous structures in high resolution. By comparing the surface of the used particles with the fresh particles, the surface of the used samples was a little smoother than the fresh samples. This indicates that only slight sintering occurred for the particles after the tests. It is emphasized that no defluidization was observed in the fluidized bed reactor.

The results of BET analysis for the fresh OC and used OCs are shown in Table 5. The specific surface area of the fresh OC is 0.217 m²/g, which is higher than the areas of used OCs. This is probably due to the slight sintering of the OC particles or the blocking of fly ash generated in the coal combustion process, leading to slight decrease of the reactivity of the particles. The reason for blocking of pores by fly ash has been verified by an EDX analysis. As shown in Fig. 17, there were some Mg and K occurred at the surface of the used particles, which were not detected in the fresh particles. However, the mass fractions of Mg and K are both less than 1%.

This result indicates that some coal ash was really absorbed on the surface of the particles in the test, and the blocking of pores by fly ash has effect on the decrease of the BET area, but the effect is very limited. Moreover, it is noted that the specific surface areas for all samples (fresh and used ones) are all relatively low, but the reactivity of the OC particles was satisfactory in the tests. This can be explained by the fact that the release of oxygen is a nucleation and nuclei growth process (Hossain and de Lasa, 2010) (implying that the release of oxygen is not solely influenced by the surface structure of the particles). Fig. 18 shows the crushing strength of used OCs for different operation time. The mechanical strength was kept well during the continuous operation, and the average crushing strengths in all tests were higher than 1 N, which was hard enough for operation in the fluidized bed.

5. Conclusions

In this study, the natural copper ore as OC of the CLOU processes was evaluated. Compared to the synthetic OC, natural copper ore has advantages such as low cost and rich supply. The oxygen uptake/release tests with different reactor temperatures were first carried out. It was found as a general trend that both the oxygen release and uptake rates increase with the reactor temperature. At a temperature ranging from 900 °C to 950 °C, the OC may operate with fast oxygen release and uptake with a slight agglomeration/sintering which easily occur for the copper ore.

The copper ore is potentially suitable for long-term use in the CLOU process of anthracite. Its reactive performance stabilizes after the first redox test. The effects of reactor temperature, superficial fluidization velocity, OC to fuel ratio, coal particle size, and steam content in fluidization gas on the coal conversion rate, coal combustion efficiency, and gas yields were then investigated in a batch-operating CLOU unit. It was found that the reaction rate increased with the fuel-reactor temperature. The reactor temperature of 900 °C was selected as the appropriate CLOU temperature as a slight agglomeration/sintering occurred at 950 °C. The carbon conversion rate decreased with the increase of superficial
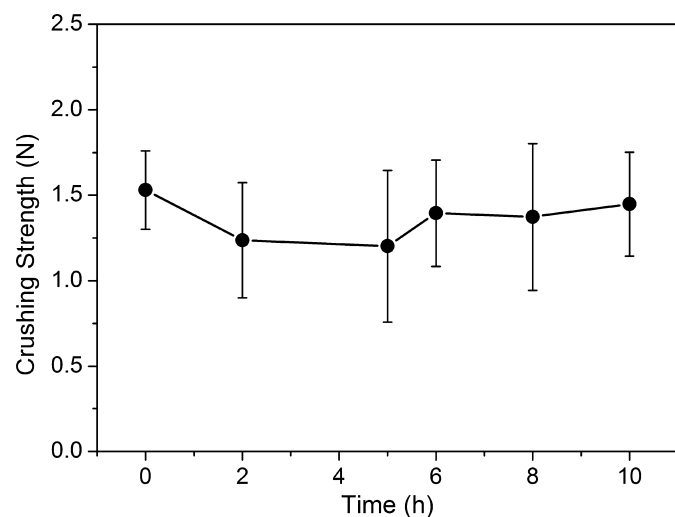

Fig. 18. Crushing strength as a function of operation time.

fluidization velocity partially due to fast, large bubbles rising through the reactor; on the contrary, the conversion rate increased with the OC to fuel ratio. For coal particle size, it was found that the reaction rate decreased notably when coal particle diameter exceeded 0.3 mm. When steam was introduced into the fluidization gas, reaction rate was accelerated significantly, which may be attributed to the fast gasification of coal char reacting with steam. In addition, although the combustion efficiency and yield of CO_2 varied considerably in different series of the tests, high combustion efficiency (more than 95%) and CO_2 yield (more than 0.96) were attained.

During the oxygen release tests and CLOU tests under appropriate experimental conditions, only slight agglomeration and sintering of the OC particles were observed. According to the XRD analysis, CuO and $CuFe_2O_4$ were the main phase composition of the OC in both of fresh and used OCs. No serious decrease of the crushing strength of the particles was observed during the 10-h operation.

Acknowledgments

References

Abad, A., Adanez, J., Garcia-Labiano, F., de Diego, L.F., Gayan, P., 2010. Modeling of the chemical-looping combustion of methane using a Cu-based oxygen-carrier. Combust. Flame 157, 602–615.

Abad, A., Adanez-Rubio, I., Gayan, P., Garcia-Labiano, F., de Diego, L.F., Adanez, J., 2012. Demonstration of chemical-looping with oxygen uncoupling (CLOU) process in a 1.5 kW(th) continuously operating unit using a Cu-based oxygen-carrier. Int. J. Greenhouse Gas Control 6, 189–200.

Adanez-Rubio, I., Gayan, P., Garcia-Labiano, F., de Diego, L.F., Adanez, J., Abad, A., 2011. Development of CuO-based oxygen-carrier materials suitable for chemical-looping with oxygen uncoupling (CLOU) process. Energy Procedia 4, 417–424.

Adanez-Rubio, I., Gayan, P., Abad, A., de Diego, L.F., Garcia-Labiano, F., Adanez, J., 2012a. Evaluation of a spray-dried $CuO/MgAl_2O_4$ oxygen carrier for the chemical looping with oxygen uncoupling process. Energy Fuels 26, 3069–3081.

Adanez-Rubio, I., Abad, A., Gayan, P., de Diego, L.F., Garcia-Labiano, F., Adanez, J., 2012b. Identification of operational regions in the chemical-looping with oxygen uncoupling (CLOU) process with a Cu-based oxygen carrier. Fuel 102, 634–645.

Adanez-Rubio, I., Abad, A., Gayan, P., de Diego, L.F., García-Labiano, F., Adanez, J., 2013. Performance of CLOU process in the combustion of different types of coal with CO_2 capture. Int. J. Greenhouse Gas Control 12, 430–440.

Adanez, J., Cuadrat, A., Abad, A., Gayan, P., de Diego, L.F., Garcia-Labiano, F., 2010. Ilmenite activation during consecutive redox cycles in chemical-looping combustion. Energy Fuels 24, 1402–1413.

Adanez, J., Abad, A., Garcia-Labiano, F., Gayan, P., de Diego, L.F., 2012. Progress in chemical-looping combustion and reforming technologies. Prog. Energy Combust. Sci. 38, 215–282.

Arjmand, M., Azad, A.M., Leion, H., Lyngfelt, A., Mattisson, T., 2011. Prospects of Al_2O_3 and $MgAl_2O_4$-supported CuO oxygen carriers in chemical-looping combustion (CLC) and chemical-looping with oxygen uncoupling (CLOU). Energy Fuels 25, 5493–5502.

Arjmand, M., Keller, M., Leion, H., Mattisson, T., Lyngfelt, A., 2012. Oxygen release and oxidation rates of $MgAl_2O_4$-supported CuO oxygen carrier for chemical-looping combustion with oxygen uncoupling (CLOU). Energy Fuels 26, 6528–6539.

Azimi, G., Leion, H., Mattisson, T., Lyngfelt, A., 2011. Chemical-looping with oxygen uncoupling using combined Mn–Fe oxides, testing in batch fluidized bed. Energy Procedia 4, 370–377.

Berguerand, N., Lyngfelt, A., 2008. Design and operation of a 10 kW(th) chemical-looping combustor for solid fuels – testing with South African coal. Fuel 87, 2713–2726.

Cuadrat, A., Abad, A., de Diego, L.F., Garcia-Labiano, F., Gayan, P., Adanez, J., 2012. Prompt considerations on the design of chemical-looping combustion of coal from experimental tests. Fuel 97, 219–232.

Fan, L.S., Zeng, L., Wang, W.L., Luo, S.W., 2012. Chemical looping processes for CO_2 capture and carbonaceous fuel conversion – prospect and opportunity. Energy Environ. Sci. 5, 7254–7280.

Figueroa, J.D., Fout, T., Plasynski, S., McIlvried, H., Srivastava, R.D., 2008. Advances in CO_2 capture technology – the US department of energy's carbon sequestration program. Int. J. Greenhouse Gas Control 2, 9–20.

Gayan, P., Adanez-Rubio, I., Abad, A., de Diego, L.F., Garcia-Labiano, F., Adanez, J., 2012. Development of Cu-based oxygen carriers for chemical-looping with oxygen uncoupling (CLOU) process. Fuel 96, 226–238.

Hossain, M.M., de Lasa, H.I., 2010. Reduction and oxidation kinetics of $Co-Ni/Al_2O_3$ oxygen carrier involved in a chemical-looping combustion cycles. Chem. Eng. Sci. 65, 98–106.

IPCC, 2008. Mitigation of Climate Change. Contribution of Working Group III to the Fourth Assessment Report of the Intergovernmental Panel on Climate Change. Cambridge University Press, Cambridge, UK.

Ishida, M., Jin, H., 1996. A novel chemical-looping combustor without NO_x formation. Ind. Eng. Chem. Res. 35, 2469–2472.

Leion, H., Lyngfelt, A., Mattisson, T., 2009a. Solid fuels in chemical-looping combustion using a NiO-based oxygen carrier. Chem. Eng. Res. Des. 87, 1543–1550.

Leion, H., Mattisson, T., Lyngfelt, A., 2009b. Using chemical-looping with oxygen uncoupling (CLOU) for combustion of six different solid fuels. Energy Procedia 1, 447–453.

Leion, H., Larring, Y., Bakken, E., Bredesen, R., Mattisson, T., Lyngfelt, A., 2009c. Use of $CaMn_{0.875}Ti_{0.125}O_3$ as oxygen carrier in chemical-looping with oxygen uncoupling. Energy Fuels 23, 5276–5283.

Lyon, R.K., Cole, J.A., 2000. Unmixed combustion: an alternative to fire. Combust. Flame 121, 249–261.

Mattisson, T., Lyngfelt, A., Leion, H., 2009a. Chemical-looping with oxygen uncoupling for combustion of solid fuels. Int. J. Greenhouse Gas Control 3, 11–19.

Mattisson, T., Leion, H., Lyngfelt, A., 2009b. Chemical-looping with oxygen uncoupling using CuO/ZrO_2 with petroleum coke. Fuel 88, 683–690.

Mei, D.F., Zhao, H.B., Ma, Z.J., Yang, W.J., Fang, Y.F., Zheng, C.G., 2013a. Oxygen release kinetics and mechanism study on Cu-, Co-, Mn-based oxygen carrier. J. Fuel Chem. Technol. 41, 235–242.

Mei, D.F., Zhao, H.B., Ma, Z.J., Zheng, C.G., 2013b. Using the sol–gel-derived $CuO/CuAl_2O_4$ oxygen carrier in chemical looping with oxygen uncoupling for three typical coals. Energy Fuels 227, 2723–2731.

Moldenhauer, P., Ryden, M., Mattisson, T., Lyngfelt, A., 2012. Chemical-looping combustion and chemical-looping with oxygen uncoupling of kerosene with Mn- and Cu-based oxygen carriers in a circulating fluidized-bed 300 W laboratory reactor. Fuel Process. Technol. 104, 378–389.

Ryden, M., Lyngfelt, A., Mattisson, T., 2011a. Combined manganese/iron oxides as oxygen carrier for chemical looping combustion with oxygen uncoupling (CLOU) in a circulating fluidized bed reactor system. Energy Procedia 4, 341–348.

Ryden, M., Lyngfelt, A., Mattisson, T., 2011b. $CaMn_{0.875}Ti_{0.125}O_3$ as oxygen carrier for chemical-looping combustion with oxygen uncoupling (CLOU)-experiments in a continuously operating fluidized-bed reactor system. Int. J. Greenhouse Gas Control 5, 356–366.

Shen, L.H., Wu, J.H., Xiao, J., 2009. Experiments on chemical looping combustion of coal with a NiO based oxygen carrier. Combust. Flame 156, 721–728.

Shulman, A., Cleverstam, E., Mattisson, T., Lyngfelt, A., 2009. Manganese/iron, manganese/nickel, and manganese/silicon oxides used in chemical-looping with oxygen uncoupling (CLOU) for combustion of methane. Energy Fuels 23, 5269–5275.

Shulman, A., Cleverstam, E., Mattisson, T., Lyngfelt, A., 2011. Chemical-looping with oxygen uncoupling using Mn/Mg-based oxygen carriers – oxygen release and reactivity with methane. Fuel 90, 941–950.

Siriwardane, R., Tian, H., Simonyi, T., Poston, J., 2013. Synergetic effects of mixed copper–iron oxides oxygen carriers in chemical looping combustion. Fuel 108, 319–333.

Son, S.R., Kim, S.D., 2006. Chemical-looping combustion with NiO and Fe_2O_3 in a thermobalance and circulating fluidized bed reactor with double loops. Ind. Eng. Chem. Res. 45, 2689–2696.

Wang, B.W., Yan, R., Zhao, H.B., Zheng, Y., Liu, Z.H., Zheng, C.G., 2011. Investigation of chemical looping combustion of coal with $CuFe_2O_4$ oxygen carrier. Energy Fuels 25, 3344–3354.

Wen, Y.Y., Li, Z.S., Xu, L., Cai, N.S., 2012. Experimental study of natural Cu ore particles as oxygen carriers in chemical looping with oxygen uncoupling (CLOU). Energy Fuels 26, 3919–3927.

Xiong, K., Zheng, G.S., 2013. Process mineralogy and flotation kinetic of a copper oxide ore during sulfuration flotation. Adv. Mater. Res. 634, 3460–3465.